

Effect of Stacking and Redox State on Optical Absorption Spectra of Melanins—Comparison of Theoretical and Experimental Results

Klaus B. Stark*

Accelrys Incorporated, 1042 Kress Street, Houston, Texas 77020

James M. Gallas

Department Physics and Astronomy, University of Texas at San Antonio, San Antonio, Texas 78249

Gerry W. Zajac and Joseph T. Golab

BP Research Center, P.O. Box 3011, Naperville, Illinois 60566-7011

Shirley Gidanian, Theresa McIntire, and Patrick J. Farmer

Department of Chemistry, University of California, Irvine, Irvine, California 92697

Received: July 23, 2004; In Final Form: November 12, 2004

In this work the effect of aggregation and oxidation on the optical absorption of eumelanin oligomeric sheets is investigated by applying quantum mechanics and atomistic simulation studies to a simplified eumelanin structural model that includes 1–3 sheets of hexameric oligomer sheets. The oligomeric hypothesis is supported by AFM characterizations of synthetic eumelanins, formed by auto-oxidation or electrochemical oxidation of dihydroxyindole (DHI). Comparison of calculated absorption spectra to experimental spectra demonstrates a red shift in absorption with oxidation and stacking of the eumelanin and validates the theoretical results.

Introduction

Melanin is the biopolymer that accounts for much of the coloration in nature.^{1,2} In humans it is responsible for the color of the hair, skin, and eyes, which span a range that includes red, yellow, brown, and black.^{3,4} Yet, the optical absorption spectra corresponding to these colors have a common feature: a broadband, structure-less curve that is a monotonically increasing function of energy.⁵

This feature may reflect an efficient mechanism for photo-protection by selective filtration of light: the wavelengths of light are filtered in proportion to their probability to damage tissue.⁶ For example, the absorption spectrum of melanin is roughly similar to the action spectrum for retinal damage; this damage has been associated specifically with macular degeneration.⁷

There is also evidence that the shape of the absorption spectrum of melanin changes with age in the retinal pigment epithelium behind the retina, specifically becoming bleached with loss of red-end absorption.⁸ In effect, after bleaching the spectrum becomes more similar in shape to the action spectrum for retinal damage.

The shape of the absorption spectrum of melanin also appears to relate to skin cancer in a particular way.⁹ People with red hair have a greater risk of skin cancer from exposure to sunlight. The type of melanin in the skin of people with red or blonde hair is called phaeomelanin and has a relatively lower optical absorption in the red end of the visible spectrum, similar to melanin that has been bleached or oxidized. Thus, the shape of

the melanin absorption spectrum may be efficient with regard to protection against major diseases in humans.

Theoretical work on melanin and its possible proto-molecules is relatively sparse due to the size of the molecules involved and the unknown nature of the overall melanin structure. Early molecular orbital calculations on monomer units predicted molecular properties, such as electron donor and acceptor qualities, in accord with experimental data known for the polymer.¹⁰ Bolivar-Martinez et al. performed *ab initio* and semiempirical calculations on different monomers, indole-quinone (IQ) and the reduced forms, semiquinone (SQ), and hydroquinone (HQ).¹¹ Calculations were performed for both the neutral molecules and singly and doubly charged anions, and the optical absorption spectra of monomeric eumelanin structures were discussed.

In previous work we performed density functional theory (DFT) calculations on the monomer of neutral IQ and its reduced forms, HQ and SQ.¹² Five possible dimers of the dihydroxyindole units were also considered and optimized. From the optimized structures absorption spectra were calculated using configuration interaction (CI) schemes and a semiempirical Hamiltonian. The results agreed well with earlier theoretical work¹¹ as well with published experimental work.¹³

A similar approach was undertaken by Bochenek and Gudowska-Nowak.¹⁴ In their work oligomers were constructed from a random composition of the same basic monomers. Semiempirical quantum mechanics calculations were performed to obtain the electronic spectra for a melanin-representing model that reproduced features of the experimental absorption spectrum of synthetic melanins. In a separate work the effect of monomer stacking on the electronic structure was investigated.¹⁵ Recently, Il'ichev and Simon¹⁶ demonstrated that several tautomerization

* To whom correspondence should be addressed. E-mail: kstark@accelrys.com.

equilibria for HQ and IQ should be considered in the complex mechanism of the oxidation of IQ and that solvent polarity has a pronounced effect on intermediate stability.

However, it is now well established that eumelanins form covalently bound "proto-molecules" consisting of sheets of indolic monomers. Beginning with extensive wide-angle X-ray scattering (WAXS) experiments^{17,18} and analyses that defined a local sheetlike structure, subsequent scanning tunneling microscopy (STM)^{19–21} and atomic force microscopy (AFM)²² studies were able to identify the local structure as the fundamental melanin units. Such proto-molecules were described as nanometer-sized stacks of 3.4-Å-spaced sheets. Further support for such structures has come from matrix-assisted laser desorption ionization (MALDI) experiments, and small-angle X-ray scattering (SAXS)²³ tests indicate that melanin is likely to consist of hydrogen-bonded aggregates of these proto-molecules.

We therefore simulated the optical spectra of melanin using a particular structural model that assumes a polyquinone layer or sheet of four to six monomers with the carbonyl residing along the perimeter of the nanometer-sized oligomers.²⁴ A continuing problem is that quantum mechanical calculations yield spectra with several discrete absorbance bands, whereas the melanin spectrum is, to a large extent, continuous. However, structural heterogeneity is inherent in the molecular structure and molecular weights of the oligomers of natural melanins. Thus, we proposed that the smooth optical absorption for melanin is obtained by superposition of all the constituent absorptions.

The structural models used in the previous work were limited to single-sheet oligomers that ranged in size from monomer through hexamers.^{12,24} In the present work the simulations include aggregates of the oligomeric sheets as well as changes in their oxidation states. These are important considerations for several reasons. A variety of experimental probes point to extensive stacking of oligomers in eumelanin—to an average of 4–5 sheets.^{19,21,25} On the other hand, several investigations support a single-sheet model for pheomelanins,²⁶ which have much lower absorbance in the visible region.

Changes in subunit oxidation state is relevant as the darkening and bleaching of melanin has been correlated to oxidation/reduction reactivity and is believed to be essential in its natural physiological functions.²⁷ It is therefore of great interest to evaluate the proto-molecule model for melanin by simulating its optical properties for oligomeric sheets in various oxidation states and to compare such spectra with the experimental data.

We previously reported a correlation between the heights of nanometer-sized melanin particles and the optical absorption in the red end of the spectrum.¹⁹ Specifically, the nominal heights of eumelanin particle was reduced from 15 to about 5 Å when the sample solutions were oxidized with hydrogen peroxide.^{19,21,25} Thus, extended oxidation causes a destacking which decreases the relative optical absorption in the red part of the optical spectrum of melanin.

Natural melanins are highly heterogeneous mixtures containing dihydroxyindole (DHI), 5,6-dihydroxyindole-2-carboxylic acid (DHICA), and other subunits, protein substituents, and absorbed metals. However, in this work we will consider only the simplest components that define the main characteristics of eumelanin, derived from DHI subunits.²⁸ Upon electrochemical oxidation DHI polymerizes on the surface of electrodes, which facilitates its handling and chemical characterization. DHI–melanin's electrochemical behavior and speciation has been described in the literature.^{28,29} The results of theoretical calculations are compared to experimental spectra of DHI–melanin,

and the rationale for the model is verified by AFM imaging. Because stacking likely varies with oxidation state and thus may be an important structural feature, extended simulations of the optical spectra for both reduced and oxidized melanin at various levels of stacking were performed. Quantum mechanics and atomistic simulation studies are applied using new structural models that include 1–3 sheets of hexameric model systems.

Theoretical Calculations

Starting structures for the stacked oligomers were generated from the monosheet structures of ref 17 obtained by the density functional theory (DFT) optimizations. In this way, new structural models including 1–3 sheets of oligomers were built. The original model was also modified by allowing for partial and full hydrolyzation of the carbonyl function. The oligomeric nonstacked structures were optimized using the DFT program DMol³ available from Accelrys Inc.^{30,31} using the same input parameter set as in our earlier work.²⁴ Then the stacked starting structures were built as described above.

The stacked structures included up to more than 200 atoms. The system size would make DFT calculation very time-consuming. Furthermore, the interactions between the sheets are expected to be dominated by dispersion interactions, which are not accounted for in available DFT functionals. On the other hand, previous studies showed that the semiempirical formalism can lead to oligomer structures with distorted chromophores.¹² Therefore, on these starting structures molecular dynamics (MD) calculations were performed using the classical simulation engine Discover³² and the COMPASS force field,^{33–37} both available from Accelrys Inc. A script³⁸ has been used to run series of MD simulations in the NVT ensemble at decreasing temperature from 800 to 300 K in steps of 50 K. The simulations were run for 200 ps using a time step of 1 fs. The resulting structures were reoptimized after each temperature step, and in this way a series of structures, which were often very close in total energy, were obtained.

On selected structures from these MD runs absorption spectra were calculated using the pair excitation configuration interaction (PECI) method^{39,40} and the AM1 Hamiltonian⁴¹ as implemented in the semiempirical program VAMP,⁴² available from Accelrys Inc. In the PECI method excited states are calculated by including all single and double excitations in which a complete electron pair is promoted. This is a very economical and effective CI expansion for closed-shell molecules and is used in VAMP for the calculation of spectra or hyperpolarizabilities. In the current calculations the number of orbitals, which have been included in the PECI expansion, varied with the number of sheets in the model (see below).

In previous investigations of the effect of oligomer size on the optical spectra it was found that the optical absorption for longer wavelengths increased with oligomer size.²⁴ To focus this work on the effects of stacking and redox state on the simulated optical spectra the oligomer size is held constant at hexamers, which was suggested by previous WAXS experiments as the smallest common oligomeric size in natural melanins^{17,18} and was the largest system studied in ref 24.

Experimental Section

Materials and Methods. The reagent 5,6-diacetoxyindole (DAI) was obtained from TCI America, Portland, OR. Water used in all experiments was 18 MΩ/cm³ Nanopure water. HPLC-grade isopropyl alcohol was purchased from Merck. All other chemicals were reagent-grade quality. Absorbance spectra were obtained on a Hewlett-Packard 8453 UV–vis spectrometer

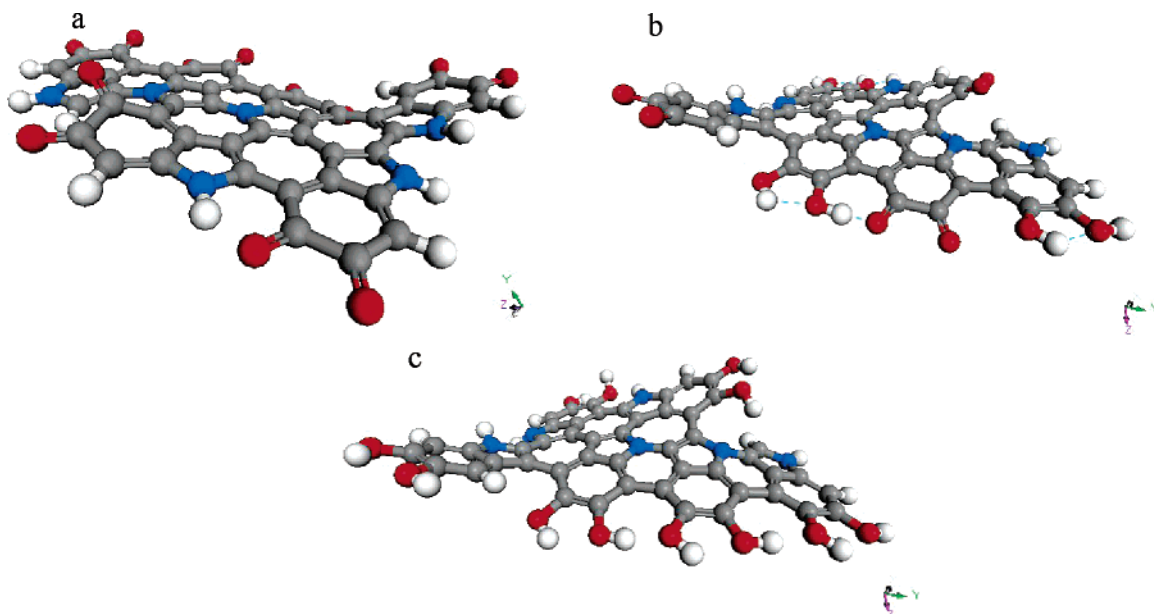


Figure 1. DFT-optimized hexameric DHI melanin structures: (a) oxidized form; (b) half-reduced form; (c) fully-reduced form. Carbon atoms are displayed in gray, oxygen atoms in red, nitrogen atoms in blue, and hydrogen atoms in white.

or a Cary 500 UV–vis–NIR spectrophotometer. Electrochemical measurements were conducted with a BAS-100B-W electrochemical analyzer using a three-electrode voltammetric cell with a platinum counter electrode and Ag/AgCl as reference electrode.

Electrochemical DHI Melanin Deposition and Characterization. Preparations of DHI melanin were performed in a glovebox under a nitrogen atmosphere. A sample of DAI (0.030 mmol, 6.0 mg) was dissolved in 12.5 mL of degassed ethanol to which 2 equiv of 0.1 M NaOH (0.55 mL) was added. This solution was allowed to stand for 1 h and then diluted to 25 mL with 0.05 M, pH 7.0 phosphate buffer. Thick films of DHI melanin were deposited on the electrode surface using cyclic voltammetric scans varying between -0.40 and 0.35 V vs Ag/AgCl for 15 cycles at a sweep rate of 50 mV s^{-1} .

The spectroelectrochemical methodology is described in detail elsewhere;²⁹ briefly, a thick melanin film was deposited on ITO plate and placed in a three-neck, anaerobic UV–vis cell containing pH 7.0 buffer solution. After obtaining the absorbance spectrum of the film without applied potential as a reference the ITO electrode was connected to the electrochemical analyzer as working electrode, using a platinum wire as counter electrode and an Ag/AgCl reference electrode. Variable potentials were applied to the film, and the absorbance spectrum of the film was obtained. Subtraction of the reference spectrum from these spectra provided the background-subtracted spectra.

Preparation of DHI Melanin Samples for AFM Examination. To prepare auto-oxidized DHI melanin, stock solutions of synthetic DHI–melanin were prepared by hydrolysis of 120 mg (0.5145 mmol) of 5,6-diacetoxyindole (DAI) with 20% molar excess of KOH (1.28 mmol) in 250 mL of deionized water. The reaction mixture was stirred rapidly in air, allowing auto-oxidation of the hydrolysis product 5,6-dihydroxyindole (DHI). The stock solution was then degassed and stored under a flow of purified N_2 presaturated with water. The stock solution was diluted 100-fold in 1:4 2-propanol/water, and 10 μ L of the resulting melanin solution was deposited onto a freshly cleaved highly oriented pyrolytic graphite (HOPG) surface, previously mounted on stainless steel pegs by double-stick tabs. The samples were allowed to dry overnight before analysis by AFM.

Electrochemical deposition of DHI melanin on HOPG was

carried out by either bulk electrolysis or cyclic voltammetry of a DHI solution using freshly cleaved HOPG as the working electrode. A DHI solution was prepared by hydrolyzing DAI in situ: DAI (0.030 mmol, 6.0 mg) was dissolved in 12.5 mL of degassed ethanol to which 2 equiv of 0.1 M NaOH (0.55 mL), needed to hydrolyze the acetoxy groups, was added. This solution was allowed to stand for 1 h and then diluted to 25 mL with pH 7.0, 0.05 M phosphate buffer. Polymerization of DHI on HOPG surface was achieved by either bulk electrolysis at 20 mV for 6 s or cyclic voltammetry for three cycles at a sweep rate of 500 mV s^{-1} for potentials varying between -0.40 and 0.35 V vs Ag/AgCl. The plates were then rinsed with deionized water and allowed to dry overnight.

AFM images were collected on a Park Scientific AutoProbe microscope operating in noncontact mode, equipped with NCAFM probe head. In a typical procedure a piezoelectric scanner with a range to 10 μ m was used for all images. The scanner was calibrated in the xy directions using a 1.0 - μ m grating and in the z direction using conventional height standards. The tips used were V-shaped silicon 2 μ m cantilevers (Ultralevers, model ULNC-AUNM, Park Scientific Instruments). The oscillation amplitude and z direction set point were adjusted to avoid tip–sample contact according to operating procedure for noncontact mode imaging. All measurements were performed in air at ambient pressure and humidity. Images were stored as 256×256 point arrays and analyzed using AutoProbe image processing software supplied by Park Scientific Instruments.

Results

Theoretical Calculations on Eumelanin. In previous work an oligomeric model of eumelanin was developed using the fully oxidized form of melanin.²⁴ Here, this chemical model is extended by including half-reduced and fully-reduced proto-molecules as well as the oxidized form. These were built starting from the optimized oxidized form obtained earlier, and the nonstacked new oligomers were optimized using similar DFT procedures.²⁴

Shown in Figure 1 are the resulting energy-optimized hexamers for the three oxidation states. For the oxidized form

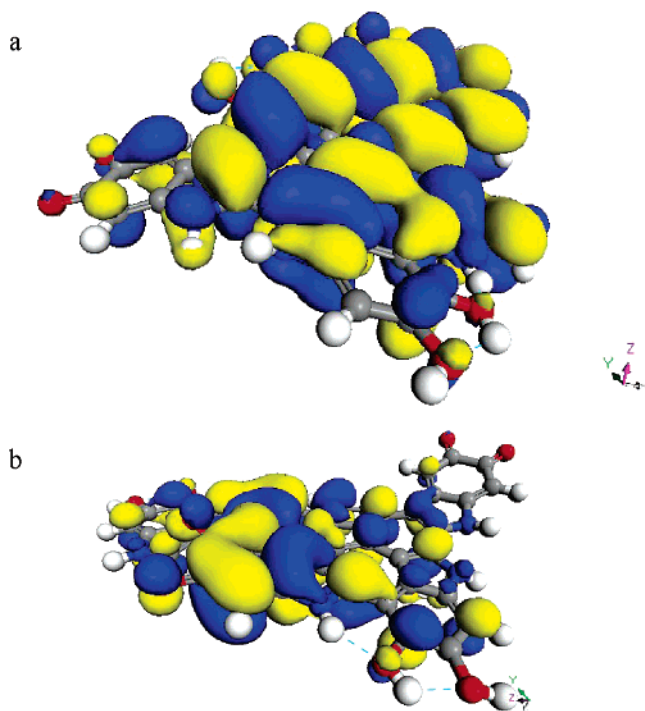


Figure 2. Frontier orbitals of the half-reduced hexamer of Figure 1b calculated with VAMP: (a) HOMO, (b) LUMO. Positive orbital lobes displayed in blue; negative orbital lobes displayed in yellow.

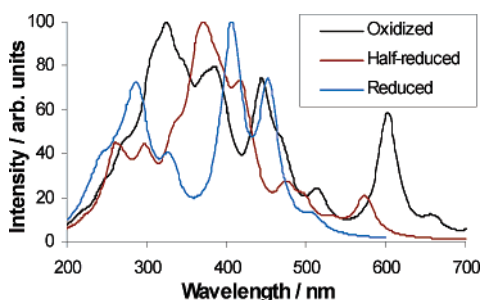


Figure 3. Lorentzian broadened calculated absorption spectra for single-sheet hexamers of the oxidized, half-reduced, and fully-reduced melanin proto-molecules.

(Figure 1a) two hydrogen-bond interactions are found which include a strong $N-H$ interaction ($r = 1.69 \text{ \AA}$) and a weak $O-H$ interaction ($r = 2.19 \text{ \AA}$). Naturally, more hydrogen bonds can form for the half-reduced form (Figure 1b) and the fully-reduced form (Figure 1c) between adjacent hydroxyl groups or between the hydrogen bond of a hydroxyl group and the adjacent carbonyl oxygen. For the half- and fully-reduced structures it is expected that hydrogen bonds will form both intra- and intersheet and that this manifold of possible hydrogen-networked isomers will affect the absorption spectra. This effect will be less pronounced for the oxidized form (vide infra).

Frontier orbitals (calculated with VAMP) are displayed for the half-reduced form in Figure 2, which shows the highest occupied molecular orbital (HOMO, Figure 2a) and the lowest occupied molecular orbitals (LUMO, Figure 2b). The HOMO has π -character and is extensively distributed around the entire molecular system, whereas the LUMO (π^*) is more localized to the interior portions of the system and excludes for the most part the oxygen-containing groups.

Calculated absorption spectra for the single-sheet structures are shown in Figure 3. The raw theoretical spectra have been Lorentzian broadened as described previously.¹² The absorption maximum of the reduced form is red shifted as compared to

the oxidized form. The predicted absorption in the red part of the spectrum is also lower in the reduced form. The absorption spectrum of the half-reduced form exhibits intermediate behavior, with absorbance bands over a broad wavelength range.

The large number of possible hydrogen-bonding interactions precluded simple energy minimization of layered structures in the reduced and half-reduced forms; therefore, the molecular dynamics quenching technique was applied to generate a manifold of low-energy structures for the stacked oligomers. Only intrasheet hydrogen bonds are expected for the oxidized structure, and consequently, the quenching procedure led to well-defined low-energy structures in which a stacked structure is built with the individual sheets somewhat shifted against each other. An example for such a structure is shown in Figure 4a. Optical spectra were calculated for the oxidized hexamer stacked in 1–3 sheets, the results being displayed in Figure 5. In these calculations the number of orbitals used for the CI expansion has been increased with the number of sheets N , so as to maintain the sampling of energy levels at 7 eV around the HOMO–LUMO gap. This led to a CI expansion including 8, 12, and 16 orbitals for $N = 1, 2,$ and $3,$ respectively. Overall the spectra become more red shifted and smooth with increasing number of sheets N . A qualitatively very similar picture (not shown in Figure 5) was obtained with a constant CI expansion into 10 orbitals for all N . These spectra, albeit different in details, showed the same trend in red shift with increasing number of sheets.

The variable CI expansion used to generate absorption spectra in Figure 5 is certainly justified when comparing the effect of stacking because it reflects the clustering of more energy levels at the same energy interval with increasing N . However, we can only be concerned with qualitative effects here since, first, our model for eumelanin is only approximate and still incomplete and, second, with increasing size of the model estimating the convergence of the CI expansion becomes more and more difficult due to the increased clustering of orbitals mentioned above. Therefore, for the absorption spectra in the other figures of this work the CI expansion is reduced to include only 10 orbitals, which reduces the computational effort while still reflecting the same general trends.

Examples of low-energy structures of hexamers of the half-reduced and reduced form obtained by the quenching procedure are shown in Figure 4b and c, respectively. Several structures exhibited very similar total energies, and typically 4–8 structures were found in a narrow energy range of 10–20 kcal/mol. Therefore, it is assumed that more than one structure contributes to the absorption spectrum of the half-reduced and reduced form. Calculated absorption spectra for selected low-energy structures of the half-reduced and reduced forms are shown in Figure 6. To generate these spectra the number of sheets was held constant at $N = 3$, following the model generated by WAXS data on enzymatically derived melanin,^{17,18} and also keeping the calculation time reasonable. In addition, the CI expansion was reduced to include only 10 orbitals (see discussion of Figure 5 above).

Synthetic Eumelanin. Melanin samples from DHI were prepared by both auto-oxidation and electrochemical deposition. Cyclic voltammograms of both forms is similar in that a sharp irreversible oxidation wave is observed with a peak current of ca. +100 mV vs Ag/AgCl, with a much weaker broad reduction current seen in the opposite scan direction (Supporting Information, Figure S1).

Figure 7 shows an AFM image and the particle size distribution of submonolayer eumelanin deposited by electro-

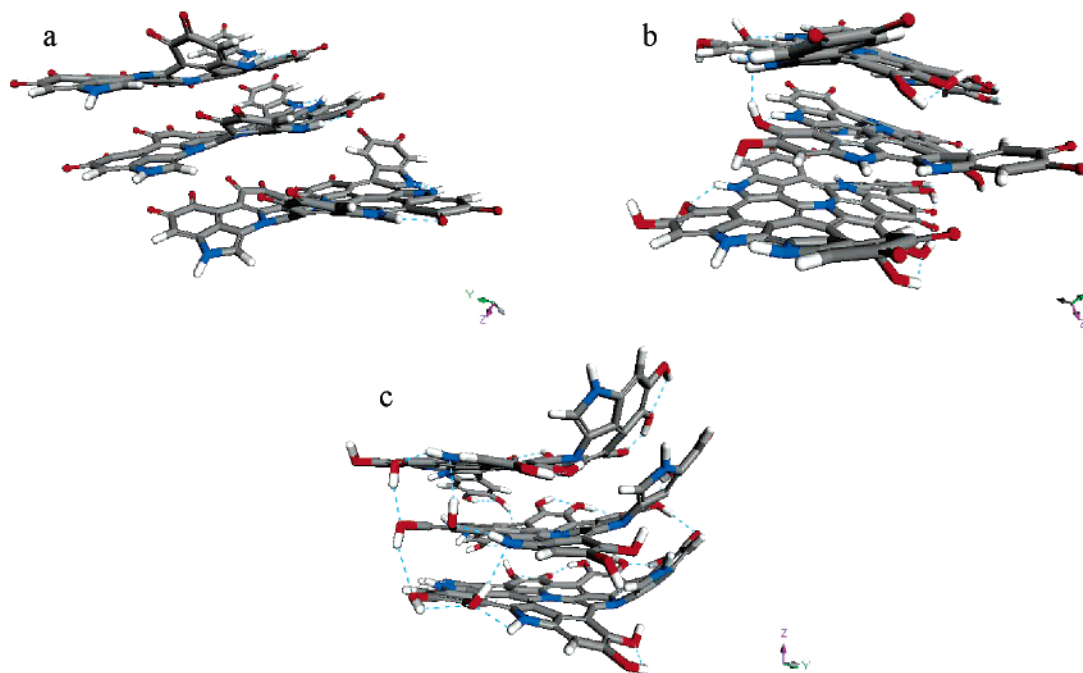


Figure 4. Low-energy structures for the three sheets of hexamers of the (a) oxidized, (b) half-reduced, and (c) reduced forms. For clarity, the structures are displayed in stick representation. Hydrogen bonds are displayed as light blue dashed lines.

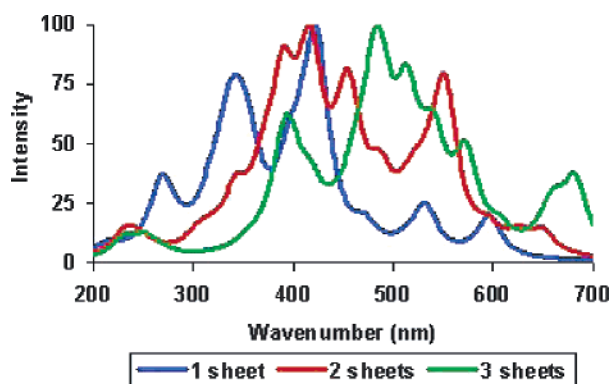


Figure 5. Lorentzian broadened and normalized calculated absorption spectra for hexamers of the oxidized form. Displayed are the spectra of the nonstacked form (1 sheet) and stacked forms with 2 and 3 sheets (for more details see text).

chemical oxidation of DHI on HOPG. Analysis gives the average particle height as 27.93 Å (standard deviation of 8.19 in a sample of 207 particles measured). The particles show a tendency to align at step edges of HOPG. By comparison, AFM imaging of colloidal melanin prepared from DHI auto-oxidation identified particles ranging from 7 to 22 Å in height, with few larger particles up to 35 Å seen (Supporting Information, S2). Statistical analysis gave the average particle height as 13.83 Å (standard deviation of 4.51 in a sample of 204 particles measured). Imaging of the micrometer-thick DHI depositions is also indicative of granularity of roughly the same scale, as illustrated in Figure 8. Note that due to the much larger size of the AFM probe tip, the lateral dimensions in these images do not correspond to the lateral sizes of the particles themselves; only the height relative to the HOPG substrate can be measured accurately.

The absorbance spectra obtained by electrolysis of a thick DHI melanin film at various potentials is shown in Figure 9. As the potential of the film is altered from its fully-reduced state at -300 mV, the absorbance increases above 400 nm with increasing potential. Between -300 and 50 mV an isosbestic point at ca. 417 nm is maintained, which denotes a simple

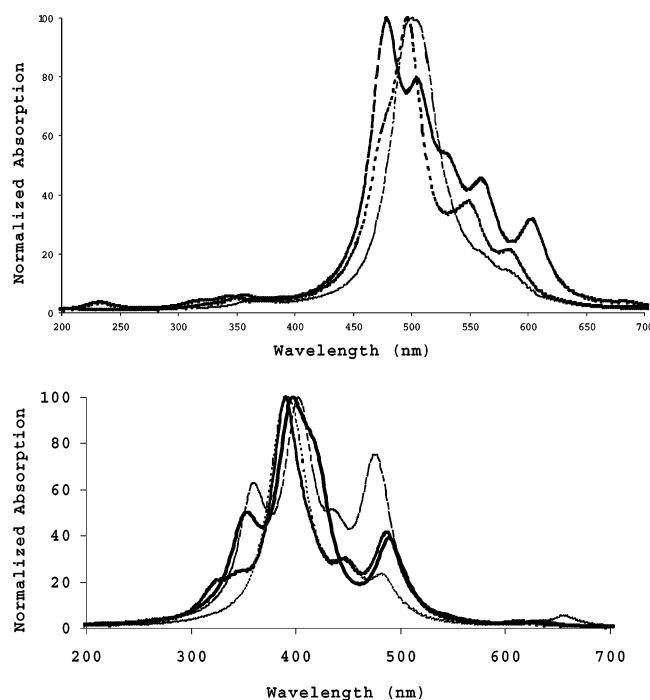


Figure 6. Absorption spectra of low-energy structures of hexamers of the half-reduced (upper panel) and reduced forms (lower panel). The number of sheets for all structures considered is held constant at $N = 3$.

interconversion of stable species. Under anaerobic conditions this absorbance change is reversible and can be repeated several times. The resting potentials of an as-made film are generally in the range of 0–50 mV, i.e., within the chemically reversible region. At potentials in the range from +50 to +300 mV the characteristic increase at 500 nm continues but the reversibility is lost, indicating a change in the chemical composition. Thick DHI melanin films treated with hydrogen peroxide display similar absorbance changes, Supporting Information, S3, but the isosbestic point at ca. 417 nm is lost almost immediately.

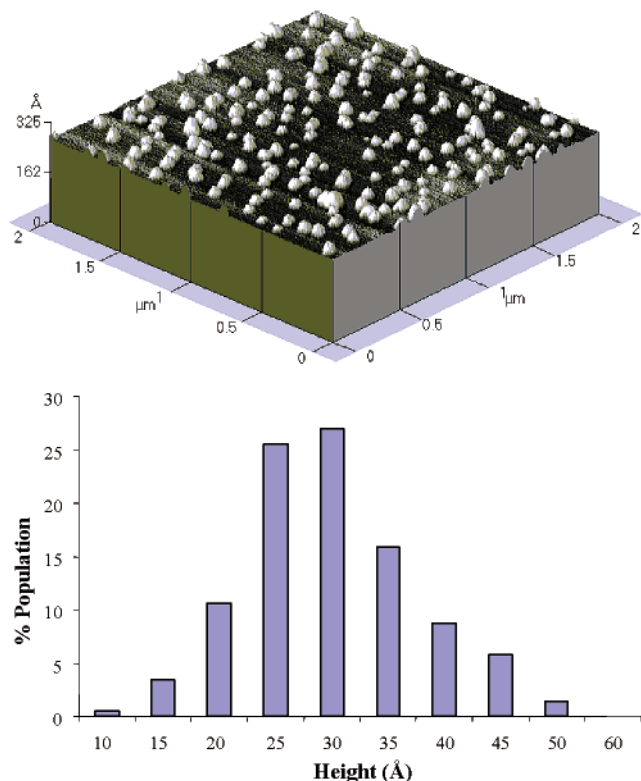


Figure 7. (Top) AFM image of DHI melanin prepared by cyclic voltammetry on HOPG. (Bottom) Histogram of percent population vs height for DHI melanin particles. Statistical analysis of 10 separate regions, $N = 207$.

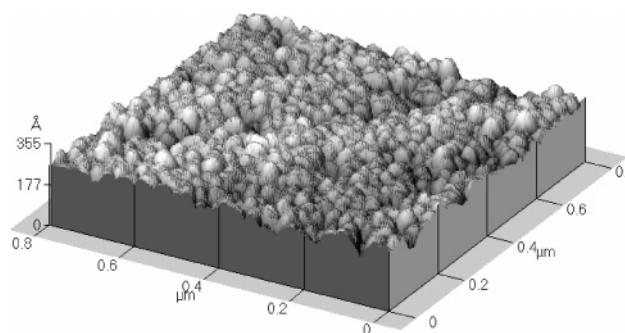


Figure 8. AFM image of thick DHI melanin film prepared by cyclic voltammetry on HOPG.

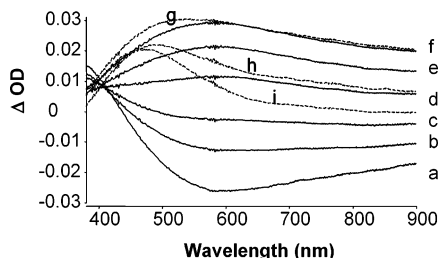


Figure 9. Changes in the optical absorption spectra of a thick DHI-melanin film on ITO during electrochemical oxidation from -300 mV; spectra taken after redox equilibration at (a) -300 , (b) -100 , (c) -50 , (d) 0 , (e) 50 , (f) 100 , (g) 200 , (h) 300 , and (i) 400 mV vs Ag/AgCl.

Discussion

In our initial simulations of the optical spectra of melanin it was surprising to see discrete optical bands associated with the nanometer-sized single oligomer obtained by density functional theory calculations. How could such discrete optical bands lead to the experimental melanin absorption spectrum, well known

for its smoothness and lack of any apparent bands throughout the visible, near-IR, and near-UV region of wavelengths?

In previous work²⁴ we simulated spectra for tetrameric, pentameric, and hexameric DHI oligomers. The most striking result was that the peaks of the various oligomers shift to the red part of the spectrum with increasing oligomer size. Thus, it is possible that with sufficient heterogeneity a superposition of such spectra one could replicate the smooth melanin optical absorption. Additional heterogeneity could be due to other structural variants of a given oligomer size, for example, those resulting from substituents such as carboxylate functionalities at the oligomer periphery which are not considered here.

Structural Models of Eumelanin. AFM images of DHI melanin all show nanoscale particles; the colloidal samples have average particle heights of 13.8 Å, which match well with previous reports on synthetic melanins.^{19,21} The average height of electrochemically deposited particles is 27.9 Å (std 8.2 Å), which corresponds to 6–7 stacked sheets and roughly agrees with the ~ 2 -nm-sized molecular structures calculated in this study. Formation of bigger particles by electrochemical deposition in comparison with auto-oxidation is probably due to the difference in polymerization conditions and nucleation on HOPG surface. Complete size agreement is not to be expected given that SAXS studies have indicated various states of aggregation of stacked sheets exist in dilute solutions.²⁵

Changes in Absorbance with Oxidation. For the nonstacked oligomers (Figure 3) the absorption in the UV part of the spectrum of the reduced form is red shifted compared to the oxidized form accompanied by a reduction of the absorption in the infrared part of the spectrum. The absorbance spectrum of the nonstacked half-reduced form exhibits intermediate behavior and has peaks over the entire wavelength range.

Stacking increases the absorption in the red-end part of the spectrum and smoothes the absorption spectrum (Figure 5). For the half- and fully-reduced forms a variety of structures are expected to contribute to the absorption spectrum due a manifold of possible hydrogen networks that can form during the stacking procedure. For the half-reduced (Figure 6, top) form the stacked model exhibits less absorption in the UV spectral range accompanied by an increase of absorption on the red end of the spectrum. For the fully-reduced form (Figure 6, bottom) stacking narrows the spectral range in which the reduced form absorbs to a region of 300–500 nm.

The effect of oxidation on the absorbance of DHI-melanin was demonstrated by spectroelectrochemical measurements on a thick film on transparent ITO electrodes, which allows fine control over the redox state of the sample. The visible spectra of colloidal melanins initially darken when oxidized, which may be a result of both the oxidation state of the catecholic subunits as well as increased scattering due to aggregation. This problem is avoided using DHI-melanin film electrodes,

The calculated optical absorption spectra generally indicate a trend, as shown in Figures 3, 5, and 6, of a stronger absorption in the red end of the spectrum with higher oxidation state of the melanin. Thus, the calculations agree in general terms with the experimental observations. However, this does not prove that this particular molecular structure as utilized for these calculations is unique and that other structures would not likewise red shift with higher oxidation state. However, it is important to note that the spectral region affected by the electrochemical oxidation of melanin is very similar to those theoretically calculated for these structures (300–700 nm). We take this to indicate that the molecular structures most likely

involved are of similar size and degree of conjugation to those considered in this study.

Effect of Stacking. The effect of stacking can be discerned by comparing Figures 3 and 6. In the half-reduced hexamer (Figure 6, top) less absorption in the UV part of the spectrum is retained. Most of the absorption occurs in the range from 400 to 600 nm. For the fully-reduced form the effect of stacking is not as pronounced. However, stacking seems to narrow the spectral range in which the reduced form absorbs to a region of 300–500 nm, whereas the nonstacked form (Figure 3) also had substantial absorption below 300 nm.

The overall effect of stacking is similar to that of oxidation, red shifting the absorbance spectra of the hexameric eumelanin model systems. This may explain the broad absorbance of natural melanins that extends to the near-IR; the lack of such stacking might explain the spectra of pheomelanin, as found in the skin of people with red or blonde hair. Pheomelanin contains a high proportion of cysteine incorporated during the oxidative polymerization of L-dopa, and X-ray scattering does not indicate the average distance between sheets of 3.4 Å as in eumelanin.²⁶ Likewise, pheomelanin's absorbance drops off dramatically past 500 nm and more closely resembles that of highly oxidized DHI melanins.

Such destacking effects are likely the cause of the significant bleaching at high wavelengths seen in Figure 9. Within a specific range the oxidation of DHI melanin is chemically reversible, but beyond 100 mV the spectral changes are irreversible, indicating oxidative degradation. Overall, the oxidation of DHI melanin by hydrogen peroxide engenders similar spectral changes as observed during electrochemical oxidations, but there is an immediate loss of the isosbestic point indicating oxidative degradation of the eumelanin structures. Peroxidation of melanins has been proposed to induce ring opening of the DHI catechols forming bis-carboxylate derivatives;²⁷ such ring-opening decomposition products have been identified by mass spectrometry in both native and synthetic melanins.^{43–46} Ring-opening decomposition of a DHI oligomer would decrease its effective conjugation and likewise decrease its propensity to stack due to increased sterics and solubility.

Conclusions

In this work we limit our investigations to the effects of oxidation state and stacking for a specific hexameric DHI oligomer and attempt to generalize the calculated changes in the intensities of the bands in the appropriate wavelength regions for the simulated spectra with changes in the intensities of the experimental spectra of DHI-derived melanin. Optical absorption spectra have been calculated for hexameric models of eumelanin using a combination of DFT and force-field methods for structure optimization and semiempirical quantum mechanics for the spectra calculation. The original oligomeric model¹⁷ has been extended to include half-reduced and fully-reduced proto-molecules in addition to the fully-oxidized form.

The oligomeric hypothesis is supported by AFM characterizations of synthetic DHI-derived eumelanins. AFM imaging of these synthetic eumelanins supports the sheet-stacking model, with the auto-oxidized samples best matching the previous literature in forming mainly 3–4-sheet stacks. The electrochemically deposited eumelanins form particles consistent with higher stacks of typically 5–6 sheets.

The calculated absorption spectra have been compared to experimental spectra of eumelanin at various levels of oxidation. The calculated optical absorption spectra agree in general terms with a red shift in the absorption with higher oxidation state of

the melanin. Although this does not prove that the particular models used for the theoretical calculations are unique and that other structures would not also red shift with higher oxidation state, the agreement is an indicator that the molecular structures most likely involved in eumelanins are of similar size and degree of conjugation to those used in this work.

Stacking significantly red shifts the absorbance spectra of the hexameric eumelanin model system and likely plays a major role in the broad absorbance to the near-IR that is typical of eumelanins. Destacking, as engendered by, e.g., ring-cleavage of the DHI monomers within an oligomer sheet, can be the cause for the bleaching of the near-IR absorbance upon oxidation.

Supporting Information Available: Three supplemental figures. This material is available free of charge via the Internet at <http://pubs.acs.org>.

References and Notes

- (1) Zeise, L. In *Melanin: Its Role in Human Photoprotection*; Zeise, L., Chedekel M. R., Fitzpatrick T. B., Eds.; Kansas Valdenmar Publishing Co.: Overland Park, 1995; pp 65–79.
- (2) Sarna, T.; Swartz, H. M. In *The Pigmentary System: Physiology and Pathophysiology*; Nordlund, J. J., Boissy, R. E., King, R. A., Ortone, J. P., Eds.; Oxford University Press: New York, 1998; pp 333–358.
- (3) Koliass, N. In *Melanin: Its Role in Human Photoprotection*; Zeise, L., Chedekel, M. R., Fitzpatrick, T. B., Eds.; Kansas Valdenmar Publishing Co.: Overland Park, 1995; pp 31–38.
- (4) Pathak, M. A.; Fitzpatrick, T. In *Sunlight and Man*; Pathak, M. A., Ed.; University of Tokyo Press: Tokyo, 1974; pp 725–750.
- (5) Crippa, P. R.; Cristofaletti, V.; Romeo, N. *Biochim. Biophys. Acta* **1978**, *538*, 164.
- (6) Gallas, J. M.; Eisner, M. In *Sunlight Damage in Humans*; Giacomoni, P., Ed.; Elsevier: Amsterdam, 2001.
- (7) Young R. W. *Survey Ophthalmol.* **1988**, *32*, 252.
- (8) Boulton, M.; Docchio, F.; Daya-Barker, P.; Ramponi, R.; Cubeddu, R. *Vision Res.* **1990**, *30*, 1291.
- (9) D'Ischia, M.; Napolitano, A.; Prola, G. *Gazz. Chim. Ital.* **1996**, *126*, 783.
- (10) Pulman, A.; Pulman, B. *Biochim. Biophys. Acta.* **1961**, *54*, 384.
- (11) Bolivar-Martinez, L. E.; Galvao, D. S.; Caldas, M. J. *J. Phys. Chem. B* **1999**, *103*, 2993.
- (12) Stark, K. B.; Gallas, J. M.; Zajac, G. W.; Eisner, M.; Golab, J. T. *J. Phys. Chem. B* **2003**, *107*, 3061.
- (13) Zhang, X.; Erb, C.; Flammer, J.; Nau, W. M. *Photochem. Photobiol.* **2000**, *71*, 524.
- (14) Bockenek, K.; Gudowska-Nowak, E. *Acta Phys. Pol., B* **2003**, *34*, 2775.
- (15) Bockenek, K.; Gudowska-Nowak, E. *Chem. Phys. Lett.* **2003**, *373*, 532.
- (16) Il'ichev, Y. I.; Simon, J. D. *J. Phys. Chem. B* **2003**, *107*, 7162.
- (17) Cheng, J.; Moss, S. C.; Eisner, M.; Zschack, P. *Pigment Cell Res.* **1994**, *7*, 255.
- (18) Cheng, J.; Moss, S. C.; Eisner, M. *Pigment Cell Res.* **1994**, *7*, 263.
- (19) Zajac, G. W.; Gallas, J. M.; Cheng, J.; Eisner, M.; Moss, S. C.; Alvarado-Swaigood, A. E. *Biochim. Biophys. Acta* **1994**, *1199*, 271.
- (20) Zajac, G. W.; Gallas, J. M.; Alvarado-Swaigood, A. E. *J. Vac. Sci. Technol. B* **1994**, *12*, 1512.
- (21) Gallas, J. M.; Zajac, G. W.; Sarna, T.; Stotter, P. *Pigment Cell Res.* **2000**, *13*, 99.
- (22) Simon, J. D. *Acc. Chem. Res.* **2000**, *33*, 307.
- (23) Gallas, J. M.; Littrell, K. C.; Seifert, S.; Zajac, G. W.; Thiyagarajan, P. *Biophys. J.* **1999**, *77*, 1135.
- (24) Stark, K. B.; Gallas, J. M.; Zajac, G. W.; Eisner, M.; Golab, J. T. *J. Phys. Chem. B* **2003**, *107*, 11558.
- (25) Littrell, K. C.; Gallas, J. M.; Zajac, G. W.; Thiyagarajan, P. *J. Photochem. Photobiol.* **2002**, *77*, 115.
- (26) Nofsinger, J. B.; Weinert, E. E.; Simon, J. D. Proceedings of the 9th ECSBM Meeting, *Biospectroscopy* **2002**, *67*, 302–305.
- (27) Korytowski, W.; Sarna, T. *J. Biol. Chem.* **1990**, *265*, 12410.
- (28) Szpoganicz, B.; Gidanian, S.; Kong, P.; Farmer, P. J. *J. Inorg. Biochem.* **2002**, *89*, 45.
- (29) Gidanian, S.; Farmer, P. J. *J. Inorg. Biochem.* **2002**, *89*, 54.
- (30) Delley, B. *J. Chem. Phys.* **1990**, *92*, 508.
- (31) Delley, B. *J. Chem. Phys.* **2000**, *113*, 7756. DMol³ is available as part of Materials Studio by Accelrys Inc.
- (32) Materials Studio Discover is described at <http://www.accelrys.com/mstudio/discover.html>.

- (33) The COMPASS force field is described at http://www.accelrys.com/mstudio/ms_modeling/compass.html.
- (34) Rigby, D.; Sun, H.; Eichinger, B. E. *Polym. Int.* **1997**, *44*, 311.
- (35) Sun, H. *J. Phys. Chem. B.* **1998**, *102*, 7338.
- (36) Sun, H.; Ren, P.; Fried, J. R. *Comput. Theor. Polym. Sci.* **1998**, *8*, 229.
- (37) Bunte, S. W.; Sun, H. *J. Phys. Chem. B* **2000**, *104*, 2477.
- (38) Meunier, M. Accelrys, Inc.; Oct 2001.
- (39) Clark, T.; Chandrasekhar, J. *Isr. J. Chem.* **1993**, *33*, 435.
- (40) Clark, T. In *Recent Experimental and Computational Advances in Molecular Spectroscopy*; NATO ASI Series C; Fausto, R., Ed.; Kluwer Academic Publishers: Dordrecht, 1993; Vol. 406, p 369.
- (41) Dewar, M. J. S.; Zoebisch, E. G.; Healy, E. F.; Stewart, J. J. P. *J. Am. Chem. Soc.* **1985**, *107*, 3902.
- (42) Clark, T.; Alex, A.; Beck, B.; Burkhardt, F.; Chandrasekhar, J.; Gedeck, P.; Horn, A.; Hutter, M.; Martin, B.; Rauhut, G.; Sauer, W.; Schindler, T.; Steinke, T.; *VAMP, Version 8.0*; Accelrys Inc.: Erlangen, 2001. This version is provided as part of Materials Studio 2.1 by Accelrys Inc.
- (43) Pezzella, A.; D'Ischia, M.; Napolitano, A.; Palumbo, A.; Prota, G. *Tetrahedron* **1997**, 8281.
- (44) Bertazzo, A.; Costa, C. V. L.; Allegri, G.; Favretto, D.; Traldi, P. *J. Mass Spectrom.* **1999**, *34*, 922.
- (45) Pezzella, A.; Napolitano, A.; D'Ischia, M.; Prota, G.; Seraglia, R.; Traldi, P.; *Rapid Commun. Mass Spectrom.* **1997**, *11*, 368.
- (46) Napolitano, A.; Pezzella, A.; Prota, G.; Seraglia, R.; Traldi, P. *Rapid Commun. Mass Spectrom.* **1996**, *10*, 204.